Accepted Manuscript

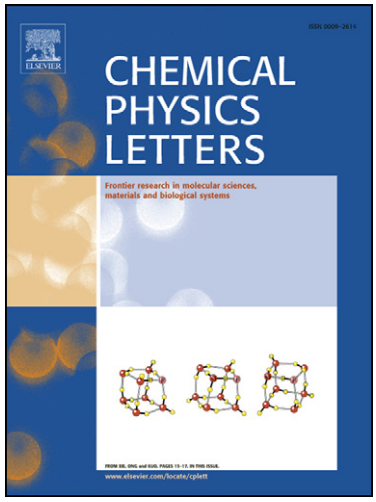

An *ab initio* study of the interaction between He and C_{36} with extrapolation to the one electron basis set limit

A.J.C. Varandas

PII: S0009-2614(08)00934-2
DOI: 10.1016/j.cplett.2008.07.014
Reference: CPLETT 26256

To appear in: *Chemical Physics Letters*

Received Date: 11 June 2008
Revised Date: 1 July 2008
Accepted Date: 3 July 2008

Please cite this article as: A.J.C. Varandas, An *ab initio* study of the interaction between He and C_{36} with extrapolation to the one electron basis set limit, *Chemical Physics Letters* (2008), doi: 10.1016/j.cplett.2008.07.014

(Submitted to *Chem. Phys. Lett.*)

An *ab initio* study of the interaction between He and C_{36} with extrapolation to the one electron basis set limit

A.J.C. Varandas*
Departamento de Química, Universidade de Coimbra
3004-535 Coimbra, Portugal

(Received June , 2008)

Abstract

The potential energy surface of exohedral He@C_{36} is analyzed in detail and extrapolated to the complete basis set limit using Möller-Plesset perturbation calculations. A limited number of coupled cluster singles and doubles calculations has also been performed. Exohedral complexes above the hexagonal faces toward the major axis are found to be the most stable, but the helium atom can move almost freely from the equator to the poles of C_{36} without dissociating the complex due to the disparity of masses. The effective $1D$ interaction potential has van der Waals attributes in good agreement with those estimated from He_2 and a Girifalco function for the C_{36} dimer, supporting three bound states.

1 Introduction

Knowledge of the pair-potentials between atoms and molecules is key for studying a number of properties, both in the gas and condensed phases. For fullerenes, they are important for understanding the physical, chemical, and mechanical properties of fullerites, including their equilibrium with the gaseous phase. [1, 2] Because accurate fullerene pair-potentials from *ab initio* electronic structure calculations are extremely hardware and computer time demanding, we have recently [3] suggested the more economical fullerene-helium interactions as probes for the former. We will examine here the hexohedral complex He@C_{36}, and use it to predict the van der Waals (vdW) attributes of the C_{36} dimer. The generality of such an approach will then be tested by considering the most abundant small fullerene after C_{60}. The method is purely *ab initio*, contrasting with other approaches where semi-empirical or empirical schemes are

*E-mail address: varandas@qtvs1.qui.uc.pt

utilized [4]. It is based on extrapolating raw *ab initio* energies computed with second-order Möller-Plesset perturbation theory (MP2) to the complete basis set (CBS) limit. An interesting asset from our method [5, 6] (the reader is referred to these papers for references to previous work) which contrasts with other approaches is that the largest required Hartree-Fock (HF) calculations are more time consuming than the MP2 ones, thus making it cost-effective and even competitive with Kohn-Sham density functional theory [7, 8] (KS-DFT) for medium size systems such as the title one.

The structure of the paper is as follows. Section 2 describes the methodology, while the results are reported and discussed on section 3. The concluding remarks are in section 4.

2 Method

A well known difficulty in *ab initio* calculations of vdW interactions is the basis set superposition error (BSSE). Correcting for this spurious attraction via counterpoise (CP) correction [9] is unaffordable for systems as large as the title one, since it implies six calculations per geometrical arrangement. However, we have demonstrated numerically [3, 10] that BSSE can be eluded in an effective way by CBS extrapolation [10]. Thus, no BSSE correction will be attempted, and we follow previous work by extrapolating separately the HF and correlation energies. For the former, we utilize the (T, Q) Karton-Martin [11] (KM) protocol, which requires raw energies calculated with triple-zeta (TZ) and quadruple-zeta (QZ) basis sets. For the correlation energy, we use the generalized uniform singlet- and triplet-pair extrapolation (GUSTE [6]) scheme where only energies for DZ and TZ (in general X_1 and X_2) basis sets are required to obtain the extrapolated energy as

$$E_{\infty}^{\mathrm{cor}} = E_{X_2}^{\mathrm{cor}} + \frac{\left(E_{X_1}^{\mathrm{cor}} - E_{X_2}^{\mathrm{cor}}\right)\left(Y_2^{-3} + \tilde{\tau}_{53} Y_2^{-5}\right)}{Y_2^{-3} - Y_1^{-3} + \tilde{\tau}_{53}\left(Y_2^{-5} - Y_1^{-5}\right)} \tag{1}$$

where $Y_i = (X_i + \alpha)$ with $i = 1, 2$, and $\alpha = -3/8$ is an offset parameter. In turn, $\tilde{\tau}_{53}$ is the unitless ratio of the triplet-pair to singlet-pair interaction coefficients [6], $\tau_{53} = A_5/A_3$, at a reference geometry. This can be determined from a fit of three correlation energies to

$$E_X^{\rm cor} = E_\infty^{\rm cor} + A_3 Y^{-3} + A_5 Y^{-5} \quad (2)$$

which requires a single calculation with a QZ basis set[†] besides the DZ and TZ ones. The calculated MP2/VQZ energy is shown in Figure 1, together with other results here reported. One obtains $\tilde{\tau}_{53} = -1.3483$, which is within 1 % of the value [3] (-1.3598) calculated for He@C_{20}. Using the latter would overestimate the total CBS extrapolated correlation energy of 6345 mE_h by less than 7 mE_h (0.1 %). As usual [6], $\tilde{\tau}_{53}$ will be assumed invariant over the full interaction potential.

3 Results and discussion

The calculations reported in this work are for He@C_{36} in the singlet ground state as MP2 calculations [12] have shown this state to be most stable for the D_{6h} isomer of C_{36} here considered. Although such studies [12] have also revealed some multireference character in the wave function, the results have shown good agreement with single-reference MP2 ones thus supporting the methodology here utilized. The Molpro suite of electronic structure programs [13] has been employed for the calculations.

Three representative orientations of the He atom relative to the center of the C_{36} structure [14] have been first considered, namely along the x, y, and z cartesian axes (cuts I, II, and III, respectively). Note that the z-axis passes on the center of the hexagonal face orthogonal to the major axis of C_{36}, while y passes on the center of a similar face but orthogonal to its minor axis. The cross sections of C_{36} viewed along such axes are displayed in the top insert of Figure 1. The calculations have been carried

[†]This has been carried out on a cluster computer at a computational cost of 247763 s per point.

using the cc-pVXZ basis set of Dunning [15] with cardinal numbers $X = D:2$, $T:3$. As required by the method, additional HF energies have been calculated with the QZ basis set. All such calculations have been done in the C_{2v} symmetry point group. To gain a better understanding of the PES, a further 1463 points have then been calculated with the DZ basis set for values of R between 4.75 and 20 Å and polar angles $0 \leq \theta/\,\mathrm{deg} \leq 90$ (colatitude) and $0 \leq \phi/\,\mathrm{deg} \leq 30$. In addition, 361 points were computed for $R = 5.8$ Å over an entire quadrant, a procedure that has also allowed to check the accuracy at symmetry related geometries. Because such calculations require C_1 symmetry and hence become too expensive, direct CBS extrapolation has not been attempted. Yet, as we shall see, such an effort can to a large extent be avoided.

Figure 1 shows the HF and MP2 calculations done for cuts I to III, while a sample of the raw calculations is presented in Table 1. In turn, Table 2 gathers the calculated vdW attributes of He@C_{36}. Unlike two noble gases, a weak vdW well due to induction forces may be expected at the HF level. However, a large fraction of it will likely be due to BSSE. As shown, the geometry of the minimum in the MP2 curves occurs innermost for cut II and outermost for cut I, in correspondence with the truncated ellipsoidal shape of C_{36}. To approximate the interaction by an effective spherically averaged potential, we may first think of treating C_{36} as a sphere of radius

$$R_m = \left(R_{m,x}^2 + R_{m,y}^2 + R_{m,z}^2\right)^{1/2} / \sqrt{3} \tag{3}$$

Using the DZ data in Table 2 leads to $R_m = 5.77$ Å. Somewhat surprisingly, this is in good agreement with the empirical estimate of (5.75 ± 0.023) Å obtained by the popular combination rule for bond distances which expresses the bond length of AB as half the sum of the A_2 and B_2 ones. Specifically, we have used $R_m = 2.99$ Å for He_2 ([10], and references therein), and $R_m = (8.55 \pm 0.02)$ Å for the C_{36} dimer as predicted from the Girifalco approach to its potential. For this, one requires the fullerene radius which has

been estimated by using [2]

$$a_n/\text{Å} = 3.55\,(n/60)^{1/2} \tag{4}$$

where n is the number of C atoms. Such a procedure yields $R_m = 8.46\,\text{Å}$ for the C_{36} dimer and $R_m = 5.72\,\text{Å}$ for $C_{36} - He$. If one uses instead the slightly modified effective radii formula [3],

$$a_n/\text{Å} = a_0 + \beta\,(n/60)^{1/2} \tag{5}$$

where $a_0 = 0.07\,\text{Å}$ and $\beta = 3.48\,\text{Å}$ are fitting parameters that were determined by imposing the commonly accepted radius of C_{60} fullerene [1] ($a_{60} = 3.55\,\text{Å}$) and approximately fitting our predicted [3] van der Waals attributes for the C_{20} dimer, the results are in the same order $R_m = 8.50\,\text{Å}$ and $5.75\,\text{Å}$. Regarding the well depth, a simple average from cuts I to III gives $\epsilon = 5.62\,\text{meV}$.

Also shown in Table 2 are the leading dispersion coefficients obtained from a fit to the correlation energies ($R \geq 6$Å). The anisotropy of the interaction is clearly reflected on their different values for different cuts. Of course, the results should be viewed with some caution as polarization functions are mostly lacking on the basis sets that were utilized to calculate the raw energies. Thus, the error bars reflect only the uncertainty due to the least-squares fitting procedure.

One-dimensional cuts for $R = 5.8\,\text{Å}$, an intermediate value for the range $5.25 \leq R/\text{Å} \leq 5.90$ where the wells occur, are shown in Figure 2. The peak at $\theta = 25$ deg corresponds to He passing over a side of the top hexagonal face for the $z \to x$ path while slightly below the crest (denoted m) is a saddle point (s″) for the $z \to y$ path. After s″, the helium atom flies along a $C - C$ bond as shown by the plateau for $50 \leq \theta/\,\text{deg} \leq 70$ lying slightly above dissociation. Topological arguments suggest two other features: a maximum m′ close to $\theta = 70$ deg (20 deg latitude), and a saddle point s″ at about $\theta = 55$ deg. Instead, in the $z \to x$ path, the helium atom feels an attraction at a similar

latitude ($\sim 55\,\mathrm{deg}$) when lying over the pentagonal face (minimum of p type), passes over a small maximum (m″) and ends at a saddle point s slightly higher in energy than p. Note that hosting He at a pentagonal face is somewhat less stable than the arrangement with He hosted at the hexagonal face orthogonal to the major axis of C_{36}. In turn, this is slightly more stable than He@C_{36} with He hosted at an hexagonal face toward the minor axis (h′). As for the equatorial motion $x \rightarrow y$, the path shows only small oscillations in energy, with equivalent minima occurring when He seats over contiguous up-oriented hexagonal faces of the host C_{36} molecule (h′ minima). Of course, there will be groups of six equivalent stationary points dictated by symmetry reasons. For example, we may predict 6 maxima m and 6 saddle points s″ in the north pole with another set of 6 of each at the south pole. Due to its cost, no numerical characterization has been done of the above stationary points by analyzing the Hessian matrix. However, Figure 3 may help on assigning their nature by showing a $2D$ (θ, ϕ) map of the potential energy globe (PEG) for the interaction at a fixed radius of $R = 5.8\,\text{Å}$.

As the PEG shows, there is no way of going from the relatively stable but rather flat equatorial minima [see the $(\theta = 90\,\mathrm{deg}, \phi)$ cut in Figure 2] to the polar minima without crossing the hills at a latitude of 30 deg or so as long as the radial coordinate is kept frozen at 5.8 Å. However, this will not be the case if R is allowed to relax such that He@C_{36} attains its minimum energy at each point (θ, ϕ). In this case, the energy landscape gets flatter with some of the above stationary points eventually ceasing to have the above characteristics. Most persist though, in particular the minima h, h′ and p and the interconnecting saddle points. As shown, the stability ordering for hosting the He atom is predicted to be h > h′ > p. Such an order remains upon CBS extrapolation. The PEG maps highlight also the symmetry and anisotropy of the interaction. Note that the He atom can circumnavigate C_{36} without dissociating, as

shown by the minimum energy path for the equator-to-pole motion in Figure 4.

Regarding CBS extrapolation, Figure 1 shows that it enhances the minima, which arise at increasingly shorter distances with basis set size. This may be rationalized as due to the fast convergence of the HF energy, although the few expensive calculations done for cut III suggest that the interaction MP2 energies are also well converged for $X = Q$. Indeed, using HF/VQZ rather than CBS/HF/VXZ energies would yield similar total energies, thus making the CBS extrapolation of the correlation energy the most important step in our method. Although the relative positioning of the minima in cuts II and III is maintained within a meV on the raw and CBS extrapolated PESs (as one would expect from the energy shifts in the well depth of 3.06 and 2.94 meV shown in Table 2 when passing from the DZ to TZ basis sets), such a deepening is less accentuated for cut I. More specifically, the CBS extrapolated minima in cuts II and III are shifted down on average by 4.5 meV (7.46 meV) with respect to the raw TZ (DZ) ones, while the corresponding shifts for cut I are 2.29 and 4.24 meV.

Another interesting result refers to well depth extracted from He_2 and the Girifalco $1D$ curve for the dimer of C_{36}, which falls between the values for cuts I and III. If Eq. (3) were utilized, one would obtain for the spherically averaged CBS curve the value of $R_m = 5.56$ Å, which is shorter by 0.20 Å (3.5 %) than the empirical value. Similarly, the above procedure would give for the well depth the value of $\epsilon = 12.06$ meV. Note, however, that the parameters of the C − C pair-potentials and the fullerene dimer [1] were optimized by matching lattice sums to solid-state data for lattice spacing and heat of sublimation, and hence may resemble more an adiabatic than a spherically averaged $1D$ curve. In fact, as already noted, the He atom can circumnavigate C_{36} adiabatically without dissociating. This is due to the disparity of masses (C_{36} is 108-144 times heavier than He), since by the Born-Oppenheimer (BO) approximation the

He atom will quickly adjust its position to feel maximum stability. Thus, the attributes of the effective $1D$ curve will be obtained under two schemes. First, by evaluating the spherically averaged potential as

$$V(R) = \int V(R,\theta,\phi)\sin(\theta)d\theta d\phi/4\pi \tag{6}$$

with the integration over the sphere for every R done with good accuracy by the trapezoidal rule. The results are satisfactorily described up to moderately repulsive energies (60 meV or so) by the effective Lennard-Jones form

$$V(R) = \epsilon\left[(R_m/R)^{2m} - 2\,(R_m/R)^{m}\right] \tag{7}$$

where $\epsilon = 3.26$ meV, $R_m = 6.14$ Å, and $m = 10.38$ are the optimum parameters obtained from a least-squares fit to the calculated MP2/VDZ spherically averaged results for $4.75 \leq R/\text{Å} \leq 8.0$. The second procedure to define the parameters of the effective $1D$ curve consists of evaluating the well depth and position as adiabatic averages along the equator-to-pole minimum energy path, which leads to $\epsilon = 4.70$ meV at $R_m = 6.03$ Å. To the above two DZ estimates, one must then add 7.46 meV (the average difference in cuts II and III from Table 2) or 6.38 meV (average difference for cuts I to III) and, similarly, subtract (0.24 ± 0.03) Å to R_m. This gives a conservative CBS extrapolated result of $\epsilon = (10.9 \pm 1.3)$ meV at $R_m = (5.83 \pm 0.04)$ Å. Finally, one must account for the lack of diffuse functions in the VXZ basis set. From the work [3] on He@C_{20}, a ratio of 0.80 has been found between the CBS well depths estimated with the VXZ basis set and the doubly diffused AVXZ one. This translates into the final estimate of $\epsilon = (13.6 \pm 1.3)$ meV. The associated Lennard-Jones curve in Eq. (7), once ϵ and R_m have been properly scaled to match such a final set of vdW parameters, is shown by the dash-dot gray line in Figure 1.

Despite being anisotropic, the BO approximation seems to support the dynamical

treatment of the $He\cdots C_{36}$ interaction as if it were governed by an effective $1D$ potential, *i.e.*, like a pseudo-diatomic molecule. Thus, we have performed vibrational calculations using the above LJ curve by treating C_{36} as a pseudo-atom of mass 432 a.m.u.. Such a procedure predicts three bound vibrational levels ($v=0,1,2$), with energies of 35, 83 and 105 cm^{-1} above the minimum. Unfortunately, to our knowledge, no data is available for comparison. Using now the vdW attributes of $He@C_{36}$ jointly with those [10] of He_2, one obtains for the C_{36} dimer $\epsilon=(195\pm39)$ meV at $R_m=(8.66\pm0.1)$ Å, which compare with the empirical values [2] of $\epsilon=188$ meV at $R_m=8.46$ Å (or $\epsilon=185$ meV at $R_m=8.50$ Å from our protocol [3]). The agreement is striking as the BO approximation suggests that such effective $1D$ potential should lie close to the adiabatic curve.

To validate the MP2 results, limited calculations have been done for cuts I to III using coupled cluster singles and doubles (CCSD) theory (the gold standard of quantum chemists) with the VDZ basis. The calculations give a T_1-diagnostic [18] of ~ 0.014 suggesting that a CCSD(T) calculation would give results close to the full CI limit. Unfortunately, because all calculations here reported had to be performed integral direct to avoid the bottleneck of storing large quantities of data on disk, no perturbative triple excitations (T) could be included. The predicted stability ordering and location of the minima are similar to those observed at MP2 level of theory. For example, the calculated CCSD well depth for cut III is $\epsilon=6.04$ meV, thus slightly shallower than the MP2 prediction. Similarly, for cut I (II), the CCSD interaction energy at $R=5.875$ Å ($R=6.125$ Å) lies 1.04 meV (0.91 meV) above the corresponding MP2 result, and we see no reason of principle why a similar trend should not be observed elsewhere. If the difference between the CBS/MP2 extrapolated estimates and the MP2/VDZ value is then added to the CCSD/VDZ result, one obtains a CBS extrapolated well depth for the effective $1D$ curve only slightly smaller than obtained by MP2 theory but essentially

within the error margins reported above. In fact, inclusion of triple excitations as in CCSD(T) may enhance the agreement.

A final remark on CPU times. As already noted, the GUSTE method required only MP2 calculations with DZ and TZ basis sets, with QZ calculations also needed for CBS extrapolating the HF energy. Typical costs (all times refer to an Intel Quad core 2.4 MHz processor) for the HF calculations carried out in C_{2v} symmetry at a point of cut III are: 1667 (DZ); 19152 (TZ); 191764 s (QZ). For the MP2 ones, the corresponding times are: 725 (DZ); 32806 s (TZ). They are roughly an order of magnitude larger in C_1 symmetry. Such HF timings fit a N^3 law in the number of basis functions (or X^9), while MP2 is expected [8] to obey N^5 (or X^{15}); CCSD is a N^6 theory. Since CBS extrapolation bears no additional cost, the expensive part will then be the TZ correlation calculations. Thus, our CBS/MP2 scheme is predictive and can be cost-competitive with KS-DFT theory. This is significant since DFT has major problems [8] with vdW interactions unless embedding empirical information [19].

4 Concluding remarks

By using the present methodology, we hope to perform accurate and predictive quantum chemistry via solution of the electronic Schrödinger equation with conventional *ab initio* methods. With multi-reference wave functions, the approach [20] [‡] can yield accurate potentials for use in reaction dynamics. If single-reference (MP2 or CCSD) theories are used, systems like He@C_{20} [3] and He@C_{36} here discussed can also be handled at costs competitive with KS-DFT. It will then be interesting to see if other interactions of relevance in biochemistry and nano-sciences can be treated similarly (see also Ref. [21]). Clearly, advances made toward more efficient MP2 methods [13,22]

[‡]Note that the offset parameter α in Eq. (1) appears with a positive sign in Ref. 20. Such a misprint has no implications on the results there reported.

and other levels of theory, as well as the joint use of density fitting [23] approximations and CBS extrapolation, provide other worth exploring avenues. The above is a major motivation of our work.

Acknowledgement

This work has the support of Fundação para a Ciência e Tecnologia, Portugal (contracts POCI/QUI/60501/2004, POCI/AMB/60261/2004, and REEQ/128/QUI/2005).

References

[1] L. A. Girifalco, J. Phys. Chem. 96 (1992) 858.

[2] V. I. Zubov, Fullerenes, Nanotubes, and Carbon Nanostructures 12 (2004) 499.

[3] A. J. C. Varandas, J. Comput. Chem. (in press).

[4] Y. K. Sung, M.-S. Son and M. S. Jhon, Inorg. Chim. Acta 272 (1998) 33.

[5] A. J. C. Varandas, J. Chem. Phys. 126 (2007) 244105.

[6] A. J. C. Varandas, J. Phys. Chem. A 112 (2008) 1841.

[7] W. Kohn and L. Sham, Phys. Rev. 140A (1965) 1133.

[8] F. Jensen, Introduction to Computational Chemistry (Wiley, Chichester, 2007), 2nd edn.

[9] F. Boys and F. Bernardi, Mol. Phys. 19 (1970) 553.

[10] A. J. C. Varandas, Theor. Chem. Acc. 119 (2008) 511.

[11] A. Karton and J. M. L. Martin, Theor. Chem. Acc. 115 (2006) 330.

[12] S. A. Varganov, P. V. Avramov, S. G. Ovchinnikov and M. S. Gordon, Chem. Phys. Lett. 362 (2002) 380.

[13] H.-J. Werner, P. J. Knowles, R. Lindh, M. Schütz, P. Celani, T. Korona, F. R. Manby, G. Rauhut, R. D. Amos, A. Bernhardsson, A. Berning, D. L. Cooper, M. J. O. Deegan, A. J. Dobbyn, F. Eckert, C. Hampel, G. Hetzer, A. W. Lloyd, S. J. McNicholas, W. Meyer, M. E. Mura, A. Nicklass, P. Palmieri, R. Pitzer, U. Schumann, H. Stoll, A. J. Stone, R. Tarroni and T. Thorsteinsson, MOLPRO, version 2002.6, a package of ab initio programs, (2003), see http://www.molpro.net.

[14] M. Feyereisen, www.ccl.net/cca/data/fullerenes/c20.cart3d.html.shtml.

[15] T. H. Dunning Jr., J. Chem. Phys. 90 (1989) 1007.

[16] A. J. C. Varandas, Adv. Chem. Phys. 74 (1988) 255.

[17] A. J. C. Varandas and J. D. Silva, J. Chem. Soc. Faraday Trans. 88 (1992) 941.

[18] T. J. Lee and P. R. Taylor, Int. J. Quantum Chem. S23 (1989) 199.

[19] T. Schwabe and S. Grimme, Acc. Chem. Research 41 (2008) 569.

[20] A. J. C. Varandas, Chem. Phys. Lett. 443 (2007) 398.

[21] J. J. Lutz and P. Piecuch, J. Chem. Phys. 128 (2008) 154116.

[22] K. Ishimura, P. Pulay and S. Nagase, J. Comput. Chem. 27 (2006) 407.

[23] H.-J. Werner, F. R. Manby and P. J. Knowles, J. Chem. Phys. 118 (2003) 8149.

Table 1: Sample raw HF/VXZ and MP2/VXZ calculations[a)] of the interaction potential between He and C_{36} in hartree.

		HF[b)]			MP2[c)]	
Cut	R[d)]	$X = D$[e)]	$X = T$[f)]	$X = Q$[g)]	$X = D$[h)]	$X = T$[i)]
I	5.0	−0.474509	−0.753230	−0.832550	−0.308529	−1.510562
	5.25	−0.476621	−0.755449	−0.834756	−0.310099	−1.512097
	5.5	−0.477531	−0.756439	−0.835750	−0.310686	−1.512646
	6.0	−0.478037	−0.757062	−0.836390	−0.310911	−1.512819
	7.0	−0.478063	−0.757181	−0.836531	−0.310823	−1.512700
II	5.0	−0.476883	−0.755495	−0.834727	−0.310625	−1.512660
	5.25	−0.477645	−0.756400	−0.835644	−0.310099	−1.512934
	5.5	−0.477966	−0.756846	−0.836106	−0.311017	−1.512967
	6.0	−0.478091	−0.757148	−0.836452	−0.310937	−1.512857
	7.0	−0.478061	−0.757183	−0.836531	−0.310820	−1.512696
III	5.0	−0.474761	−0.753335	−0.834727	−0.309013	−1.511132
	5.25	−0.476720	−0.755445	−0.834761	−0.310393	−1.512457
	5.5	−0.477596	−0.756425	−0.835738	−0.310899	−1.512915
	6.0	−0.478093	−0.757060	−0.836388	−0.311039	−1.512964
	7.0	−0.478069	−0.757184	−0.836532	−0.310841	−1.512738

[a)] Carried out in C_s symmetry. [b)] Calculated energies once added a value of 1365 E_h.. [c)] Calculated energies once added a value of 1370 E_h.. [d)] In angstrom. [e)] Energy at the asymptote (250 Å) = −1365.478060 E_h. [f)] Energy at the asymptote (250 Å) = −1365.757175 E_h. [g)] Energy at the asymptote (250 Å) = −1365.836530 E_h. [h)] Energy at the asymptote (250 Å) = −1370.310785 E_h. [i)] Energy at the asymptote (250 Å) = −1371.512630 E_h.

Table 2: vdW attributes[a] (geometry and well depth) and leading dispersion coefficients of He@C_{36}.

		R_m	ϵ	$C_6^{b)}$	$C_8^{b)}$
Cut	X	Å	meV	meV Å^{-6}	meV Å^{-8}
I	D	6.00	3.40	44±3	3169±149
	T	5.92	5.35	19±0.1	9721±5
	CBS	5.79	7.64	27±3	12630±174
II	D	5.52	6.29	31±5	3711±209
	T	5.44	9.35	82±0.1	5705±4
	CBS	5.25	13.36	121±2	6670±99
III	D	5.85	7.35	28±9	6572±552
	T	5.75	10.20	64±5	12568±264
	CBS	5.62	15.18	152±15	13245±933

[a)] From a fit to a realistic form [16]. [b)] From a fit of $E^{\rm cor}(R \geq 6\,\text{Å})$ to $-\sum_{n=6,8} C_n \chi_n(R/\rho) R^{-n}$, where $\chi_n(R/\rho)$ are damping functions [16] with the reference distance used to define the reduced coordinate taken as ρ=5.5 Å. All values are multiplied by 10^{-3}.

Figure 1: Raw (in black) and CBS extrapolated (thick curves in gray) energies for the interaction between He and C_{36}: HF (open circles); MP2 (solid dots). For a given line style, points refer downwards to $X = D$, T, and Q (pentagon). Also indicated are the empirical (diamond) and corrected CBS (xyerrorbar) estimates, LJ curve (dash-dot, gray), and cross sections of C_{36} in cuts I to III; see the text. The insert highlights the HF curves.

Figure 2: Raw HF/VDZ and MP2/VDZ energies for the He atom moving along a meridian in the zx and zy (angle$=\theta$) planes or equatorially (angle$=\phi$) on the xy plane keeping the distance to the center of fullerene fixed at $R = 5.8$ Å.

Figure 3: PEG for the interaction between C_{36} and He with $R = 6.0$ Å. Negative energies in solid and positive in dashed, with first contour at the pole starting at -7.03 meV, and the lowest at equator being -5.03 meV, all spaced by 1 meV.

Figure 4: Relaxed PEG for hexoedral He@C_{36} with the minimum energy path in dash-dot. Key as in Fig. 3, with contours equally spaced by 0.31 meV, and lowest contour at equator being -6.13 meV.

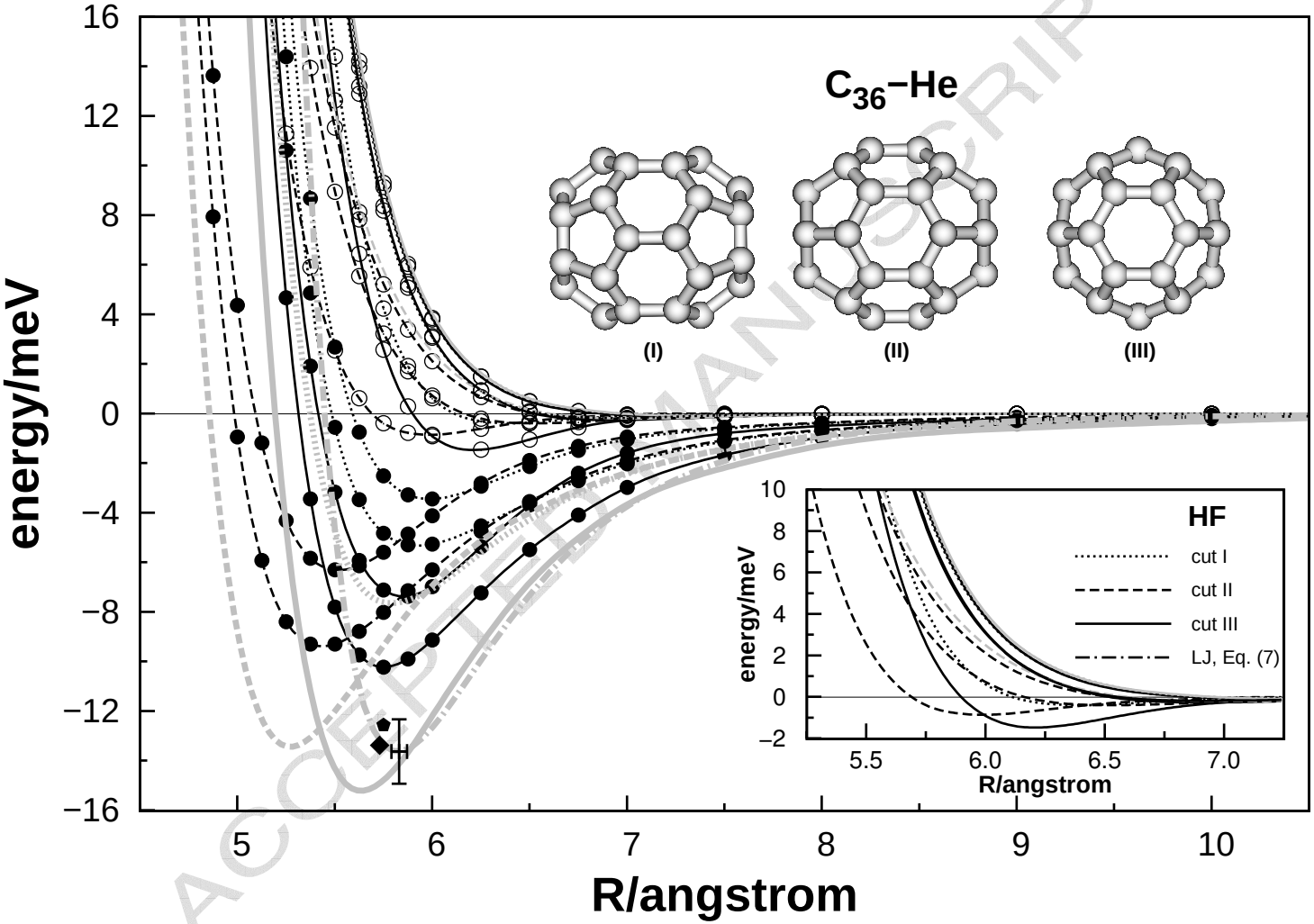

Figure 1, Varandas, Chem. Phys. Lett.

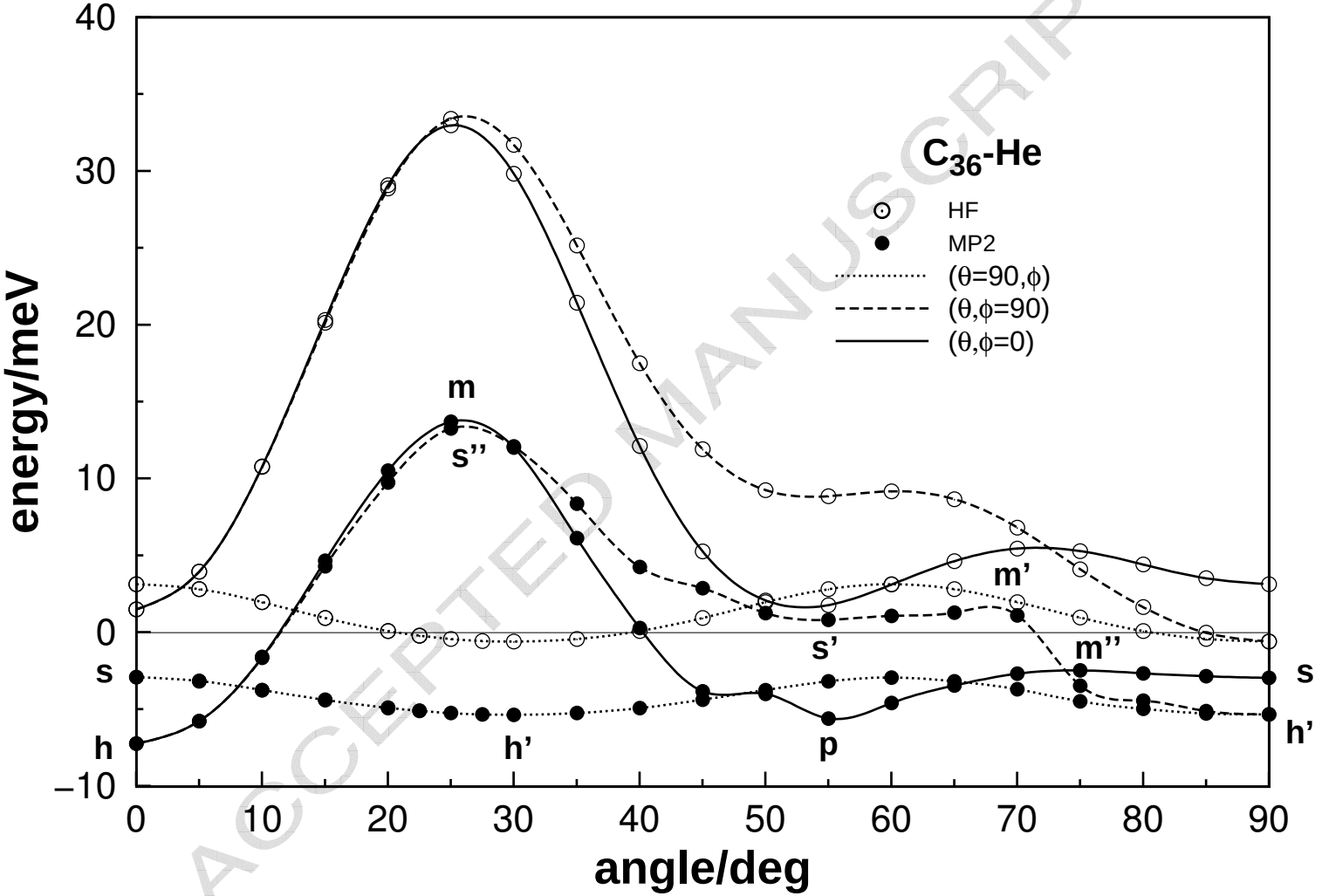

Figure 2, Varandas, Chem. Phys. Lett.

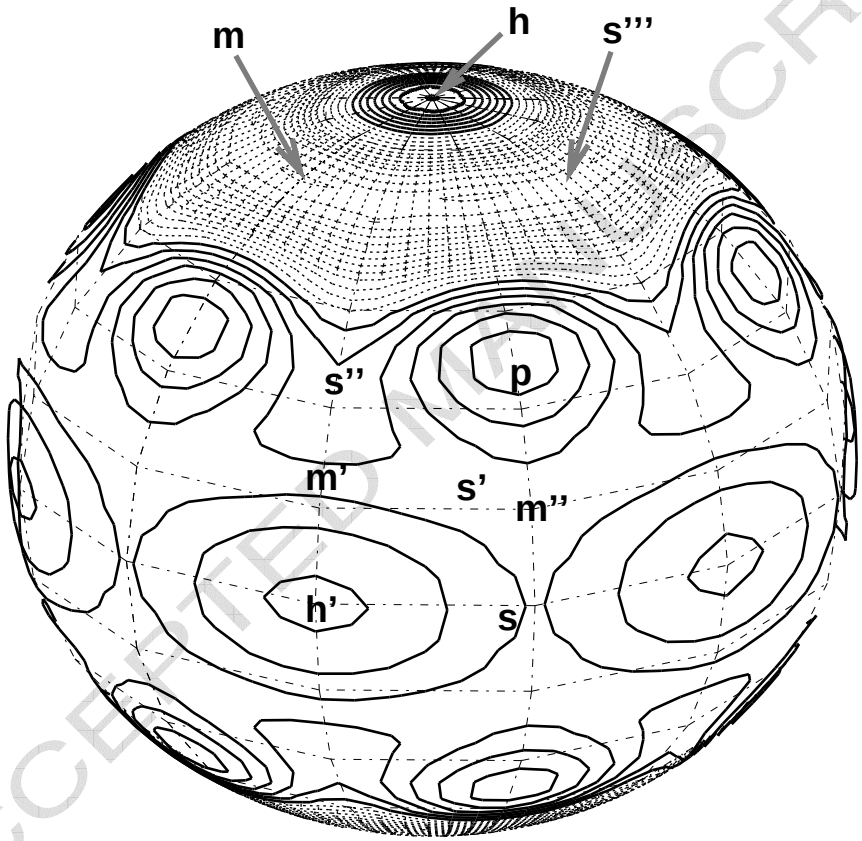

Figure 3, Varandas, Chem. Phys. Lett.

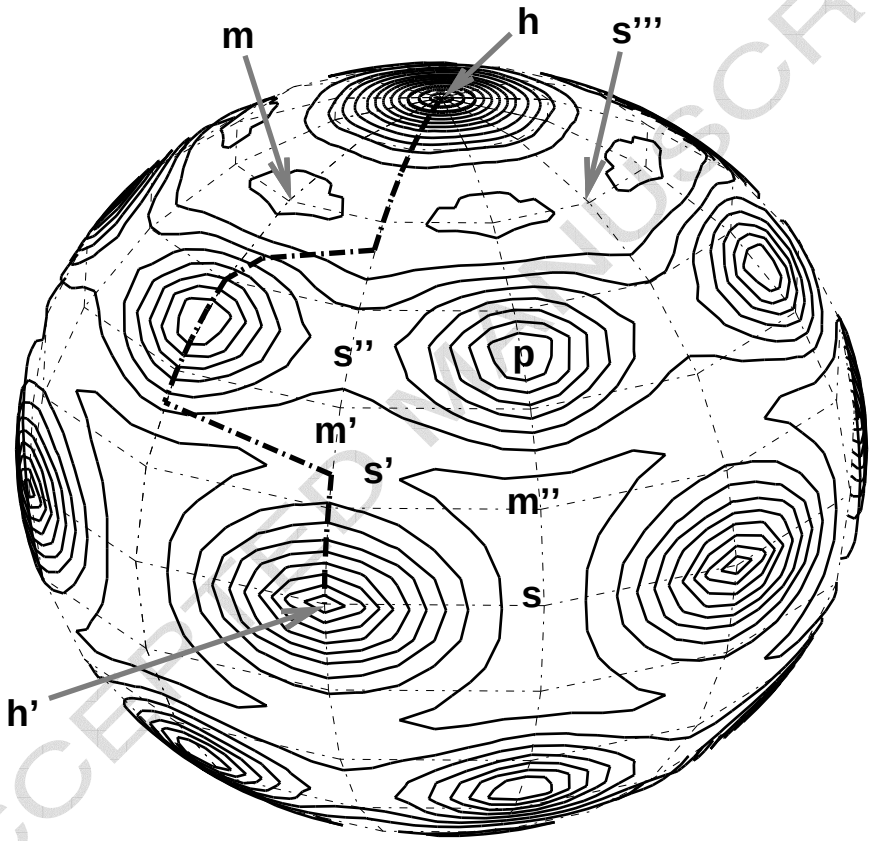

Figure 4, Varandas, Chem. Phys. Lett.

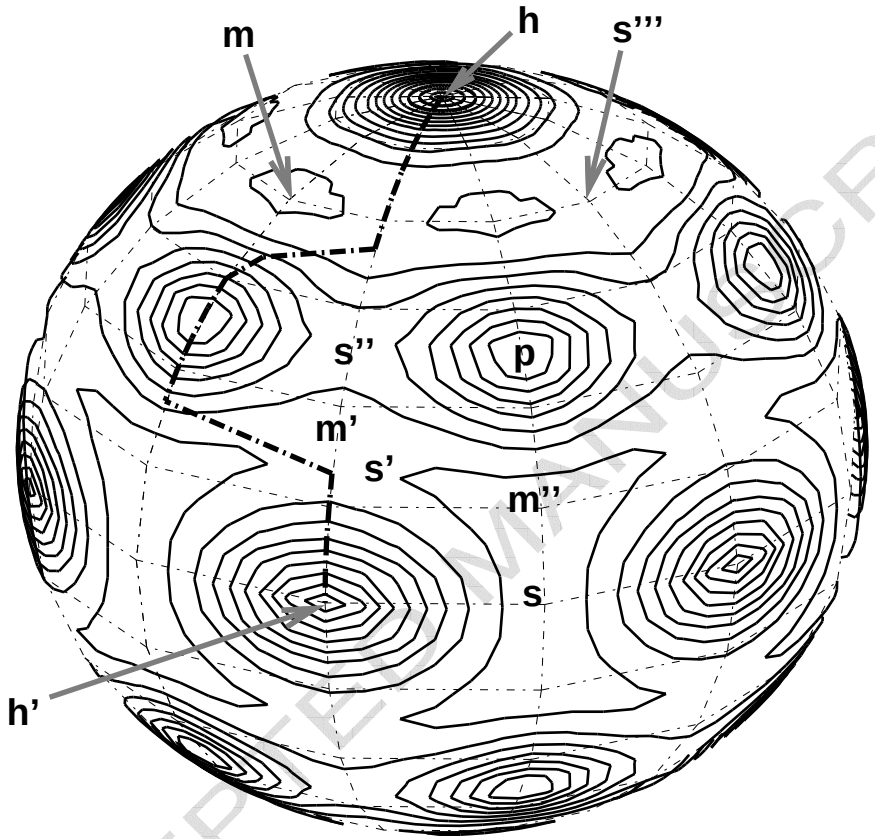

*** Graphical Abstract (pictogram)**

The potential energy surface of exohedral $He@C_{36}$ has been accurate calculated by *ab initio* methods.

*** Graphical Abstract (synopsis)**